

# Reduced transition probabilities for the $\gamma$ -decay of the 7.8 eV isomer in $^{229}\text{Th}$

Nikolay Minkov<sup>1,2,\*</sup> and Adriana Pálffy<sup>2,†</sup>

<sup>1</sup>*Institute of Nuclear Research and Nuclear Energy,*

*Bulgarian Academy of Sciences, Tzarigrad Road 72, BG-1784 Sofia, Bulgaria*

<sup>2</sup>*Max-Planck-Institut für Kernphysik, Saupfercheckweg 1, D-69117 Heidelberg, Germany*

(Dated: May 17, 2022)

The reduced magnetic dipole and electric quadrupole transition probabilities for the radiative decay of the  $^{229}\text{Th}$  7.8 eV isomer to the ground state are predicted within a detailed nuclear-structure model approach. We show that the presence and decay of this isomer can only be accounted for by the Coriolis mixing emerging from a remarkably fine interplay between the coherent quadrupole-octupole motion of the nuclear core and the single-nucleon motion within a reflection-asymmetric deformed potential. We find that the magnetic dipole transition probability which determines the radiative lifetime of the isomer is about one order of magnitude smaller than presently estimated. The so-far disregarded electric quadrupole component may have non-negligible contributions to the internal conversion channel. These findings support new directions in the experimental search of the  $^{229}\text{Th}$  transition frequency for the development of a future nuclear frequency standard.

PACS numbers: 23.35.+g, 23.20.Lv, 21.60.Ev, 21.60.Cs, 06.30.Ft

*Introduction.* From the nuclear structure point of view, the  $^{229}\text{Th}$  actinide isotope is a typical representative of a heavy nucleus with pronounced collectivity and possible presence of octupole (reflection-asymmetric) deformation [1]. The increasing interest that  $^{229}\text{Th}$  has received in the last decade beyond the nuclear physics community is due to an exceptional phenomenon: the presence of a  $3/2^+$  isomeric, i.e., long-lived, state identified at energy of approx. 7.8 eV, which appears as an almost degenerate counterpart of the  $5/2^+$  ground state [2]. This extremely small energy (the smallest known up to date in nuclear spectra) renders for the first time a nuclear transition accessible to vacuum ultra-violet (VUV) lasers. Given the very narrow linewidth of the transition and the high robustness of nuclei to external perturbations [3], the isomeric state has been proposed for novel applications such as a nuclear frequency standard with unprecedented accuracy [3–5] or a nuclear laser [6].

The first direct observation of the low-energy isomeric state decay of  $^{229}\text{Th}$  via internal conversion (IC) has been reported recently [7]. The most recent energy value of  $7.8 \pm 0.5$  eV could be determined only indirectly in a calorimetric measurement by subtraction of x-ray energy differences between neighboring levels [2]. So far, a direct excitation of the isomeric state has not been achieved [8, 9], and the radiative lifetime of the transition to the ground state could only be estimated theoretically. A nuclear structure theory prediction of the isomer energy on the eV level of accuracy is beyond reach. On the other hand, predictions for the reduced  $3/2^+ \rightarrow 5/2^+$  transition probabilities have been attempted on the basis of branching ratios (Alaga rules [10]) from the observed decays of neighboring levels [11, 12], as well as within the quasiparticle-plus-phonon model (QPM) [13] in Refs. [14, 15]. Due to the very small energy it is assumed that the magnetic dipole ( $M1$ ) dominates over

the electric quadrupole ( $E2$ ) for the transition from the isomeric  $3/2^+$  to the ground  $5/2^+$  state.

So far, the unusually low isomer energy and its decay properties are not well understood from the nuclear structure point of view. In this Letter, we report the elaboration and first-time application of a sophisticated model approach which incorporates the shape-dynamic properties together with the intrinsic structure characteristics typical for the actinide nuclei. The formalism includes a description of the collective quadrupole-octupole vibration-rotation motion of the nucleus which in the particular case of odd-mass nuclei is coupled to the motion of the single (odd) nucleon within a reflection-asymmetric deformed-shell model with pairing correlations and fully microscopic treatment of the Coriolis interaction. The model calculation determines the energy and the radiative decay properties of this isomer as integral parts of the entire low-lying positive- and negative-parity spectrum and transition probabilities observed in  $^{229}\text{Th}$ . On this basis, we show that the low-lying isomer energy emerges as the consequence of a very fine interplay between the rotation-vibration degrees of freedom and the coupling to the motion of the unpaired neutron. The predicted transition probability value  $B(M1) = 0.007$  Weisskopf units (W.u.) lies about one order of magnitude lower than the value of 0.048 W.u. deduced in Ref. [11] and by a factor of two lower than the value of 0.014 W.u. obtained from the QPM model [15]. This might offer an explanation for recent experimental difficulties to observe the radiative decay of the isomer [8, 9, 16]. The electric quadrupole value  $B(E2) = 27$  W.u. is by a factor of approx. 2 smaller than the only other available prediction in Ref. [15]. Despite the recent claims in Ref. [12] that the electric quadrupole channel is negligible for both radiative and IC decays, for excited electronic state configurations, the predicted values render the contribution

of the  $E2$  transition for IC of equal magnitude with the  $M1$  one [17]. These findings support experimental efforts under way that focus on the IC from the isomeric state [18] as opposed to experiments involving so far mostly the radiative decay of the isomer [8, 9, 16].

*Theoretical approach.* The complex nuclear structure of the  $^{229}\text{Th}$  isotope is governed by the fine interplay between the collective quadruple-octupole (QO) vibration-rotation motion of the nucleus, the single-particle (s.p.) motion of the odd, unpaired nucleon and the Coriolis interaction between the latter and the nuclear core. The collective motion is described through the so-called coherent QO mode (CQOM) giving raise to the quasi parity-doublet structure of the spectrum [19, 20], whereas the s.p. one is determined by the deformed shell model (DSM) with reflection-asymmetric Woods-Saxon (WS) potential [21] and pairing correlations of Bardeen-Cooper-Schrieffer (BCS) type included as in Ref. [22]. The Coriolis interaction between CQOM and the odd nucleon is considered following Refs. [23, 24].

The Hamiltonian of QO vibrations and rotations coupled to the s.p. motion with Coriolis interaction and pairing correlations can be written in the form

$$H = H_{\text{s.p.}} + H_{\text{pair}} + H_{\text{qo}} + H_{\text{Coriol}}. \quad (1)$$

Here  $H_{\text{s.p.}}$  is the s.p. Hamiltonian with the WS potential for axial quadrupole, octupole and higher multipolarity deformations [21] providing the s.p. energies  $E_{\text{sp}}^K$  with given value of the projection  $K$  of the total and s.p. angular momentum operators  $\hat{I}$  and  $\hat{j}$  on the intrinsic symmetry axis.  $H_{\text{pair}}$  is the standard BCS pairing Hamiltonian [25]. Together they yield the quasi-particle (q.p.) spectrum  $\epsilon_{\text{qp}}^K$  as shown in Ref. [22].  $H_{\text{qo}}$  represents oscillations of the even-even core with respect to the quadrupole ( $\beta_2$ ) and octupole ( $\beta_3$ ) axial deformation variables mixed through a centrifugal (rotation-vibration) interaction [20].  $H_{\text{Coriol}}$  involves the Coriolis interaction between the even-even core and the unpaired nucleon (see Eq. (3) in [20]). It is treated as a perturbation with respect to the remaining part of (1) and then incorporated into the QO potential of  $H_{\text{qo}}$  defined for given angular momentum  $I$ , parity  $\pi$  and s.p. band-head projection  $K_b$  which leads to a joint term [24]

$$H_{\text{qo}}^{IK_b} = -\frac{\hbar^2}{2B_2} \frac{\partial^2}{\partial \beta_2^2} - \frac{\hbar^2}{2B_3} \frac{\partial^2}{\partial \beta_3^2} + \frac{1}{2} C_2 \beta_2^2 + \frac{1}{2} C_3 \beta_3^2 + \frac{\tilde{X}(I^\pi, K_b)}{d_2 \beta_2^2 + d_3 \beta_3^2}. \quad (2)$$

Here,  $B_2$  ( $B_3$ ),  $C_2$  ( $C_3$ ) and  $d_2$  ( $d_3$ ) are quadrupole (octupole) mass, stiffness and inertia parameters, respectively, and  $\tilde{X}(I^\pi, K_b)$  determines the centrifugal term in which the Coriolis mixing is taken into account (see Supplementary Material [26] for details).

The Coriolis perturbed wave function for the QO spectrum built on a q.p. state with  $K = K_b$  and parity  $\pi^b$

corresponding to the Hamiltonian (1) is obtained in the first order of perturbation theory from the QO core plus particle wave function [24] (see Supplementary Material [26]). The corresponding expression for the energy has the form

$$E_{nk}^{\text{tot}}(I^\pi, K_b) = \epsilon_{\text{qp}}^{K_b} + \hbar\omega \left[ 2n + 1 + \sqrt{k^2 + b\tilde{X}(I^\pi, K_b)} \right], \quad (3)$$

where  $b = 2B/(\hbar^2 d)$  denotes the reduced inertia parameter and  $n = 0, 1, 2, \dots$  and  $k = 1, 2, 3, \dots$  stand for the radial and angular QO oscillation quantum numbers, respectively, with  $k$  odd (even) for the even (odd) parity states of the core [27]. The levels of the total QO core plus particle system, determined by a particular  $n$  and  $k^{(+)}$  ( $k^{(-)}$ ) for the states with given  $I^{\pi=+}$  ( $I^{\pi=-}$ ) form a split (quasi) parity-doublet [28]. Furthermore,  $\omega = \sqrt{C_2/B_2} = \sqrt{C_3/B_3} \equiv \sqrt{C/B}$  stands for the frequency of the coherent QO oscillations [19, 20].

Having the Coriolis perturbed wave function we were able to calculate the reduced probabilities  $B(E1)$ ,  $B(E2)$ ,  $B(E3)$  and  $B(M1)$  for transitions between initial (i) and final (f) states with energies given by Eq. (3) (see Supplementary Material [26] for the explicit expressions). We note that the reduced transition probability expression contains first-order and second-order  $K$ -mixing effects. First-order mixing terms practically contribute with non-zero values only in the cases  $K_{i/f} = K_\nu = 1/2$ , i.e., when a  $K_{i/f} = 1/2$  band-head state is mixed with another  $K_\nu = 1/2$  state present in the considered range of admixing orbitals above the Fermi level. A second order mixing effect connects states with  $\Delta K = 1, 2$  and allows different combinations of  $|K_i - K_f| \leq 2$  which provide respective non-zero contribution of the Coriolis mixing to the transition probability. Therefore, non-zero transition probabilities between states with different  $K$ -values are rendered possible. Thus, unlike stated in previous works [11, 12], in our model *it is the Coriolis interaction which allows the otherwise forbidden  $M1$  and  $E2$  inter-band isomeric transition to occur.* This allows us to examine in detail the *capability of such a complete nuclear structure mechanism to provide a prediction for the isomer decay in  $^{229}\text{Th}$*  based on the interaction between collective and s.p. degrees of freedom in the nucleus.

*Numerical results.* We applied the above CQOM-DSM approach to the low-lying part of the experimental  $^{229}\text{Th}$  spectrum [29] including positive- and negative-parity levels with energy below 400 keV as shown in Fig. 1. We suggest that this is enough to constrain the CQOM model parameters as to provide reliable predictions for the unknown  $B(E2)$  and  $B(M1)$  transition probabilities between the isomeric  $3/2^+$  and the  $5/2^+$  ground state. This spectrum is interpreted according to CQOM as consisting of two parity quasi-doublets as follows.

The lower, yrast (yr) quasi-doublet, is built on the  $K_{\text{bYr}} = 5/2^+$  ground state corresponding to the  $5/2[633]$

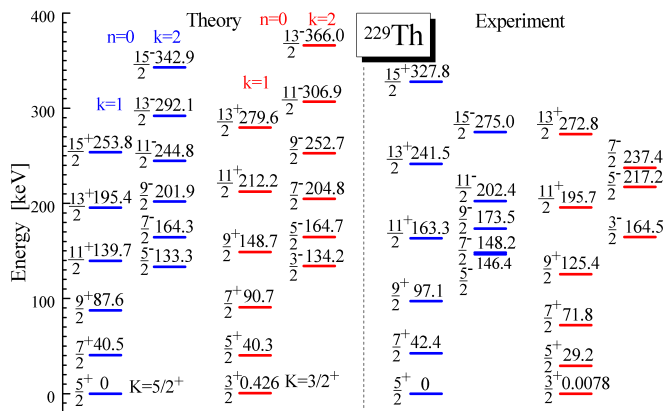


FIG. 1: Theoretical and experimental quasi parity-doublet levels of  $^{229}\text{Th}$ . The CQOM model parameters used are  $\omega = 0.20$  MeV/ $\hbar$ ,  $b = 0.28$   $\hbar^{-2}$ ,  $d_0 = 18$   $\hbar^2$ ,  $c = 79$ ,  $p = 1$  and  $A = 0.158$  keV. See text for further explanations. Experimental data from Ref. [29].

Nilsson s.p. orbital. The set of positive- and negative-parity levels is interpreted as collective rotations and coherent vibrations of the QO deformed core-plus-particle system. The parity splitting is due to the QO vibration mode characterized by the lowest value of the radial-oscillation quantum number  $n = 0$ , the lowest possible angular-oscillation number  $k_{\text{yr}}^{(+)} = 1$  for the positive-parity sequence and one of the few lowest possible  $k_{\text{yr}}^{(-)} = 2, 4, 6$  values for the negative-parity states.

The upper, excited (ex), i.e., non-yrast, quasi parity-doublet is built on the isomeric  $K_{b\text{ex}} = 3/2^+$  state corresponding to the  $3/2[631]$  Nilsson s.p. orbital. For other nuclei, the first non-yrast quasi-doublet is usually associated with the higher radial-vibration mode,  $n = 1$  [28]. However, having in mind the practically full degeneracy of the pair of  $5/2^+$  and  $3/2^+$  states, here we consider that this doublet also corresponds to the collective QO mode characterized by  $n = 0$  with the lowest  $k_{\text{ex}}^{(+)} = 1$  and one of the lowest possible  $k_{\text{ex}}^{(-)} = 2, 4, 6, 8$ .

Thus, we have two similar collective quasi-doublet structures with  $n = 0$ ,  $k_{\text{yr}}^{(+)} = k_{\text{ex}}^{(+)} = 1$ , built on the two quasi-degenerate s.p. states. This theoretical supposition is supported by the observation that both the yrast and non-yrast experimental positive-parity sequences have very similar level spacings up to  $I = 13/2^+$  and only differ by a mutual shift. The latter can be explained by the different  $K_b$ -values in the centrifugal term  $\tilde{X}(I^\pi, K_b)$  in Eq. (2) leading to a relative down-shift of the  $5/2^+$  sequence with respect to  $3/2^+$  [26]. The experimental negative-parity sequences in both quasi-doublets, though not looking as similar as the positive-parity ones, are also reasonably placed in this scheme suggesting equal or close values of  $k_{\text{yr}}^{(-)}$  and  $k_{\text{ex}}^{(-)}$ .

The calculations were made for several combinations of  $k_{\text{yr}}^{(-)}$  and  $k_{\text{ex}}^{(-)}$  values providing respective sets of ad-

justed CQOM model parameters as detailed in the following. We consider the lowest values  $k_{\text{yr}}^{(-)} = k_{\text{ex}}^{(-)} = 2$  as the basic set providing the lowest-energy QO vibration mode. On the other hand the calculation with higher  $k^{(-)}$ -values allows us to examine the stability of the obtained predictions against different model conditions.

We have first determined the quadrupole ( $\beta_2$ ) and octupole ( $\beta_3$ ) deformations in DSM by requiring that the orbitals  $5/2[633]$  and  $3/2[631]$  appear in the neutron s.p. spectrum as the last occupied and first not occupied orbitals, respectively, and the spacing between them is as small as possible. By varying  $\beta_2$  between the experimental values 0.2301(39) and 0.2441(15) known for the neighboring even-even nuclei  $^{228}\text{Th}$  and  $^{230}\text{Th}$ , respectively [30], and changing additionally  $\beta_3$  we obtained  $\beta_2 = 0.240$  and  $\beta_3 = 0.115$ . It is important to note that we found the correct placing and mutual spacing of both orbitals *at non-zero octupole deformation*.

In the following, starting from the set of  $k_{\text{yr}}^{(-)} = k_{\text{ex}}^{(-)} = 2$  we performed fits of the six CQOM model parameters for fixed BCS pairing constants (see Supplementary Material [26] for details). Apart from  $\omega$  and  $b$ , further model parameters are  $d_0$ , which fixes the QO potential origin [19, 20] and together with  $\omega$  and  $b$  determines the energy levels;  $c = (B/\hbar)\omega$ , the reduced oscillator frequency, and  $p = \sqrt{(d_2 + d_3)/(2d_2)}$  which gives the relative contribution of the quadrupole mode [27], both additionally determining the transition probabilities. The sixth parameter is the Coriolis mixing strength  $A$  which determines both energies and transitions. This procedure allowed us to obtain the theoretical  $3/2^+$  isomer energy value as small as 0.4 keV. The theoretical energy levels are shown in Fig. 1 in comparison with the respective experimental data. The root mean square (rms) deviation of the predicted energy levels from the experimental ones is  $\text{rms}_{\text{yr}} = 39.9$  keV for the yrast-based band and  $\text{rms}_{\text{ex}} = 26$  keV for the isomer-based band, with the total deviation being  $\text{rms}_{\text{tot}} = 34$  keV. In this calculation the predicted  $B(E2)$  and  $B(M1)$  values for the  $3/2^+$  isomer decay are 27.04 W.u. and 0.0076 W.u. respectively. The theoretical (Th1) and experimental [31] values for the available  $B(E2)$  and  $B(M1)$  transition probabilities are compared in Table I.

Though from a nuclear physics point of view 0.4 keV is a very good approximation of the experimental 0.0078 keV, faced with atomic physics accuracy standards a refinement is desirable. Therefore, we implemented one further step by slightly varying the CQOM parameters values given in the caption of Fig. 1 to individually adjust the theoretical  $3/2^+$  isomer energy to the exact experimental value. As might be expected, this led to a slight overall deterioration of the predictions for the other energy levels, with an increase of  $\text{rms}_{\text{tot}}$  by 1 keV. At the same time the predicted  $B(E2)$  and  $B(M1)$  values slightly changed to 23.05 W.u. and 0.0061 W.u., re-

spectively. To see the effect of this  $3/2_{\text{ex}}^+$  adjustment on the other described transition probabilities we present the respective theoretical values (Th2) in Table I. The overall change in the obtained transition probabilities is small. This refinement illustrates the sensitivity of the obtained description and predictions to the model parameters in reference to the accuracies inherent for the atomic physics quantities. Also, it shows how the collective QO-oscillation mode affects the band-head energy. Further checks were performed keeping the same BCS conditions fixed for few more combinations of higher  $k_{\text{yr}}^{(-)}$  and  $k_{\text{ex}}^{(-)}$  values without tuning the  $3/2^+$  isomer energy (see Supplementary Material [26]). The predicted isomer  $B(E2)$  and  $B(M1)$  values do not change very much and vary in the limits between 20 and 30 W.u. for  $B(E2)$  and 0.006 and 0.008 W.u. for the  $B(M1)$  transition probabilities, confirming the prediction stability of the model.

TABLE I: Theoretical and where available experimental  $B(E2)$  and  $B(M1)$  transition values for the low-lying spectrum of  $^{229}\text{Th}$ . Results are given for two sets of model parameters, denoted as Th1 (corresponding to Fig. 1) and Th2 presented in the text. Experimental data from Ref. [31].

| Type | Transition  | Th1[Th2] (W.u.)        | Exp (Err) (W.u.)        |
|------|---|------------------------|-------------------------|
| E2   | $7/2_{\text{yr}}^+ \rightarrow 5/2_{\text{yr}}^+$ | 252 [267]              | 300 ( $\pm 16$ )        |
| E2   | $9/2_{\text{yr}}^+ \rightarrow 5/2_{\text{yr}}^+$ | 82 [85]                | 65 ( $\pm 7$ )          |
| E2   | $9/2_{\text{yr}}^+ \rightarrow 7/2_{\text{yr}}^+$ | 213 [224]              | 170 ( $\pm 30$ )        |
| E2   | $9/2_{\text{yr}}^+ \rightarrow 5/2_{\text{ex}}^+$ | 19.98 [17.37]          | 6.2 ( $\pm 0.8$ )       |
| E2   | $3/2_{\text{ex}}^+ \rightarrow 5/2_{\text{yr}}^+$ | <b>27.04 [23.05]</b>   | –                       |
| M1   | $7/2_{\text{yr}}^+ \rightarrow 5/2_{\text{yr}}^+$ | 0.0093 [0.0085]        | 0.0110 ( $\pm 0.0040$ ) |
| M1   | $9/2_{\text{yr}}^+ \rightarrow 7/2_{\text{yr}}^+$ | 0.0178 [0.0157]        | 0.0076 ( $\pm 0.0012$ ) |
| M1   | $9/2_{\text{yr}}^+ \rightarrow 7/2_{\text{ex}}^+$ | 0.0151 [0.0130]        | 0.0117 ( $\pm 0.0014$ ) |
| M1   | $3/2_{\text{ex}}^+ \rightarrow 5/2_{\text{yr}}^+$ | <b>0.0076 [0.0061]</b> | –                       |

*Discussion.* The model description of the low-lying positive- and negative-parity levels of  $^{229}\text{Th}$  shown in Fig. 1 provides a reasonable interpretation of the  $3/2^+$  isomeric state as a part of the quasi-doublet structure stemming from the general QO rotation-vibration degrees of freedom of the total system and the coupling between the even-even core and the motion of the unpaired neutron. Our detailed model calculations suggest that the extremely small isomer energy may be the result of a very fine interplay between all involved degrees of freedom. We emphasize the crucial importance of the Coriolis interaction for explaining the presence of an  $M1$  transition between the yrast and non-yrast band, contradicting statements in the literature on the weakness of the Coriolis mixing [11, 12]. At the same time our result corroborates with the role of the Coriolis mixing assumed in the QPM calculations [14, 15]. We note here that the present model is essentially different from the QPM application. In the latter the mean field is supposed to be

reflection symmetric, whereas the octupole mode is included as a phonon admixture to the q.p. excitation. In the present approach the quadrupole and octupole modes are treated on the same footing both in DSM and in the collective CQOM part, reflecting the present understanding about the stronger role of the octupole deformation in the shape dynamics of actinide nuclei. Furthermore, in the CQOM+DSM model the Coriolis term is not diagonalized numerically but treated explicitly within the perturbation theory providing a possibility to follow in detail the role of the  $K$ -mixing in the mechanism of isomer decay. The limits of validity of this perturbative approach were examined in Ref. [24] for the quasi parity-doublet spectra of  $^{223}\text{Ra}$  and  $^{221}\text{Fr}$ , where a much stronger Coriolis interaction is observed.

Inspection of our results in Table I shows that the experimental data is reproduced quite well with some entries like the magnetic intraband  $7/2_{\text{yr}}^+ \rightarrow 5/2_{\text{yr}}^+$  theoretical value being within the experimental uncertainties. A larger discrepancy is observed for the  $9/2_{\text{yr}}^+ \rightarrow 7/2_{\text{yr}}^+$   $M1$  transition. This might be related to the larger discrepancy (about 10 keV) of the predicted energy for the  $9/2_{\text{yr}}^+$  level compared to the one ( $\sim 2$  keV) of  $7/2_{\text{yr}}^+$  (see Fig. 1). We note that this particular transition probability is overestimated also by QPM and different experimental values are available at present [15, 31] calling for further measurements. The interband  $9/2_{\text{yr}}^+ \rightarrow 7/2_{\text{ex}}^+$   $M1$  transition in Table I shows a better agreement with the experiment, and our  $B(E2; 9/2_{\text{yr}}^+ \rightarrow 5/2_{\text{ex}}^+)$  values of 19.98 and 17.37 W.u. though overestimating the ENSDF value of 6.2 ( $\pm 0.8$ ) W.u., are both within the error bar of the experimental value of 19.2 ( $\pm 4.8$ ) W.u. reported in [15]. Thus, having in mind the possible uncertainties in the experimental data we may conclude that the present calculations provide a reasonable overall description of the electromagnetic transition properties of  $^{229}\text{Th}$ . In addition we note that CQOM provides plausible values for the intrinsic quadrupole moment within the yrast and non-yrast sequences varying in the range of 780–960 fm<sup>2</sup> for  $5/2^+ \leq I \leq 15/2^+$ , with the lower value being close to the one of 750 fm<sup>2</sup> considered in Ref. [15].

The present formalism allows to study the fine interplay between all involved dynamic modes, providing a way to exactly tune the isomer energy without essential loss of overall accuracy through the six CQOM parameters. In order to check the reliability of the predicted decay probabilities and the predictive capability of the model as a whole we have performed a similar calculation for the neighboring odd-mass isotope  $^{231}\text{Th}$  using the six parameter values obtained from the  $^{229}\text{Th}$  spectrum. We considered the yrast quasi parity-doublet band in  $^{231}\text{Th}$  together with two  $B(E1)$  transition values available from experimental data [31]. The only additional refinements we made were the (necessary) use of an effective  $E1$  charge of  $0.43e$ , with  $e$  the proton charge, and a slight shift of  $\beta_2$  in DSM from 0.24 to  $\beta_2 = 0.248$  to

obtain the last occupied orbital with  $K^\pi = 5/2^+$ . We found quite a reasonable description of both energies and  $B(E1)$  transition probabilities of  $^{231}\text{Th}$  with the energy rms value being 26 keV. Thus, we may conclude that our model parameters demonstrate rather stable behavior among different isotopes in conjunction with the concept of “sloppy” parameter fits discussed in Ref. [32].

This analysis and the good reproduction of the available values for intraband and interband transition rates suggest that the experimental transition probabilities for the  $3/2^+$ -isomer decay in  $^{229}\text{Th}$  will be found in the limits of  $B(E2)=20\text{--}30$  W.u. and  $B(M1)=0.006\text{--}0.008$  W.u. The fact that the  $B(M1)$  value is significantly smaller than the theoretical predictions up to date [11, 12, 15] is in agreement with and could be an explanation for the lack of experimental success in driving or observing the radiative channel for the isomeric transition [8, 9, 16]. At the same time the suggested range for the transition probabilities could serve as a clearly determined accuracy target for further experiments. Furthermore, we note that the  $E2$  channel, thus far disregarded, can play a role for IC, especially when considering other electronic orbitals than the neutral Th atomic ground state. Scaling the IC rates obtained in Ref. [17] using the previously available larger value  $B(M1) = 0.048$  W.u., it turns out that the  $E2$  component could even be dominant over the  $M1$  one for conversion involving the  $7p$ ,  $6d$  or  $5f$  electronic orbitals. Our new results on the  $B(E2)$  and  $B(M1)$  transition probabilities therefore support experimental efforts aiming at the determination of the isomeric decay properties via the observation of IC electrons.

This work is supported by the DFG and by the BNSF under contract DFNI-E02/6. AP gratefully acknowledges funding by the EU FET-Open project 664732.

---

\* Electronic address: nminkov@inrne.bas.bg

† Electronic address: Palfly@mpi-hd.mpg.de

[1] P. A. Butler and W. Nazarewicz, *Rev. Mod. Phys.* **68**,

- 349 (1996).  
 [2] B. R. Beck *et al.*, *Phys. Rev. Lett.* **98**, 142501 (2007); LLNL-PROC-415170 (2009).  
 [3] C. J. Campbell *et al.*, *Phys. Rev. Lett.* **108**, 120802 (2012).  
 [4] E. Peik and C. Tamm, *Europhys. Lett.* **61**, 181 (2003).  
 [5] E. Peik and M. Okhupkin, *C. R. Phys.* **16**, 516 (2015).  
 [6] E. V. Tkalya, *Phys. Rev. Lett.* **106**, 162501 (2011).  
 [7] L. von der Wense *et al.*, *Nature* **533**, 47 (2016).  
 [8] J. Jeet *et al.*, *Phys. Rev. Lett.* **114**, 253001 (2015).  
 [9] A. Yamaguchi *et al.*, *New J. Phys.* **17**, 053053 (2015).  
 [10] G. Alaga, K. Alder, A. Bohr and B. Mottelson, *Kgl. Dan. Vid. Selskab, Mat.-fys. Medd.* **29**, No. 9 (1955).  
 [11] A. Dykhne and E. Tkalya, *JETP Lett.* **67**, 251 (1998).  
 [12] E. V. Tkalya, C. Schneider, J. Jeet and E. R. Hudson, *Phys. Rev. C* **92**, 054324 (2015).  
 [13] V. G. Soloviev, *Theory of Complex Nuclei* (Pergamon Press, Oxford, 1976).  
 [14] K. Gulda *et al.*, *Nucl. Phys. A* **703**, 45 (2002).  
 [15] E. Ruchowska *et al.*, *Phys. Rev. C* **73**, 044326 (2006).  
 [16] L. von Wense, *On the direct detection of  $^{229m}\text{Th}$* , PhD Thesis, Ludwig Maximilian University Munich (2016).  
 [17] P. V. Bilous, G. A. Kazakov, I. D. Moore, T. Schumm and A. Pálffy, *Phys. Rev. A* **95**, 032503 (2017).  
 [18] B. Seiferle, L. von der Wense, and P. G. Thirolf, *Phys. Rev. Lett.* **118**, 042501 (2017).  
 [19] N. Minkov *et al.*, *Phys. Rev. C* **73**, 044315 (2006).  
 [20] N. Minkov *et al.*, *Phys. Rev. C* **76**, 034324 (2007).  
 [21] S. Cwiok, J. Dudek, W. Nazarewicz, J. Skalski and T. Werner, *Comp. Phys. Comm.* **46**, 379 (1987).  
 [22] P. Walker and N. Minkov, *Phys. Lett. B* **694**, 119 (2010).  
 [23] N. Minkov, S. Drenska, M. Strecker and W. Scheid, *J. Phys. G* **36** 025108 (2009); **37**, 025103 (2010).  
 [24] N. Minkov, *Physica Scripta* **T154**, 014017 (2013).  
 [25] P. Ring and P. Schuck, *The Nuclear Many-Body Problem*, (Springer, Heidelberg, 1980).  
 [26] see Supplementary Material [url] (2017).  
 [27] N. Minkov *et al.*, *Phys. Rev. C* **85**, 034306 (2012).  
 [28] N. Minkov *et al.*, *Phys. Rev. C* **88**, 064310 (2013).  
 [29] <http://www.nndc.bnl.gov/ensdf/>.  
 [30] T. Kibedi and R. H. Spear, *ADNDT* **80**, 35-82 (2002).  
 [31] [http://www.nndc.bnl.gov/nudat2/indx\\_adopted.jsp](http://www.nndc.bnl.gov/nudat2/indx_adopted.jsp).  
 [32] T. Niksic and D. Vretenar, *Phys. Rev. C* **94**, 024333 (2016).